Cortés López, V.; Ortiz Sánchez, MC.; Aleixos Borrás, MN.; Blasco Ivars, J.; Cubero García, S.; Talens Oliag, P. (2016). A new internal quality index for mango and its predicción by external visible and near-infrared reflection spectroscopy. Postharvest Biology and Technology. (118):148-158. doi:10.1016/j.postharvbio. 2016.04.011.

A new internal quality index for mango and its prediction by external visible and near-infrared reflection spectroscopy

Cortés, V.[1]; Ortiz, C.[2]; Aleixos, N.[3]; Blasco, J.[4]; Cubero, S.[4]; Talens, P.[1*]

[1]Departamento de Tecnología de Alimentos. Universitat Politècnica de València. Camino de Vera s/n, 46022, Valencia (Spain).
[2]Departamento de ingeniería rural y agroalimentaria. Universitat Politècnica de València. Camino de Vera s/n, 46022, Valencia (Spain).
[3]Departamento de Ingeniería Gráfica. Universitat Politècnica de València. Camino de Vera s/n, 46022, Valencia (Spain).
[4]Centro de Agroingeniería. Instituto Valenciano de Investigaciones Agrarias (IVIA). Ctra. Moncada-Náquera km. 4.5, 46113, Moncada, Valencia (Spain).

ABSTRACT

A non-destructive method based on external visible and near-infrared reflection spectroscopy for determining the internal quality of intact mango cv. 'Osteen' was investigated. An internal quality index, well correlated with the ripening index of the samples, was developed based on the combination of a biochemical property (total soluble solids) and physical properties (firmness and flesh colour) of mango samples. The diffuse reflectance spectra of the samples were recorded and used to predict the internal quality and the ripening index. These spectra were obtained using different spectroscopic external measurement sensors involving a spectrometer, capable of measuring in different spectral ranges (600-1100 nm and 900-1750 nm), and also a spectrocolorimeter that measured in the visible range (400-700 nm). Three regression models were developed by partial least squares to establish the relationship between spectra and indices. Good results in the prediction of

internal quality of the samples were obtained using the full spectral range (R_p^2 = 0.833-0.879, RMSEP = 0.403-0.507 and RPD = 2.341-2.826) and some selected wavelengths (R_p^2 = 0.815-0.896, RMSEP = 0.403-0.537 and RPD = 2.060-2.905). The results obtained from this study revealed that external visible and near-infrared reflection spectroscopy can be used as a non-destructive method to determine the internal quality of mango cv. ‘Osteen’.

Keywords: reflection spectroscopy, fruit, quality, chemometrics, non-destructive.

1. INTRODUCTION

Spain is the main European producer of subtropical fruits, with approximately 1400 ha dedicated to mango (Galán & Farre, 2005). In particular, the south-west region has a large potential for the production of tropical and subtropical fruit, with a favourable year-round climate and infrequent frosts.

Mango fruit is sold in the market in quality categories. In the past, skin colour, fruit size and shape, freedom from defects and the absence of decay were the most common quality determinants, but nowadays other organoleptic characteristics related with internal and nutritional quality play an important role in the consumer's decision, as opposed to just appearance. The quality of mangoes changes almost daily and it is essential to correlate all the major quality parameters with one another in order to reveal the overall quality of the fruit (Jha *et al.*, 2011).

In a climacteric fruit, such as mango, the fruit is not considered to be of desired eating quality at the time it initially becomes mature. It requires a ripening period before it achieves the taste and texture desired at the time of consumption. The ripening process is regulated by genetic and biochemical events that result in biochemical changes such as the biosynthesis of carotenoids (Mercadante & Rodriguez-Amaya, 1998), loss of ascorbic acid (Hernández *et al.*, 2006), increase in total soluble solids (Padda *et al.*, 2011); physical changes such as weight, size, shape, firmness and colour (Ornelas-Paz *et al.*, 2008; Kienzle *et al.*, 2011); and changes in aroma, nutritional content and flavour of the fruit (Giovannoni, 2004). Traditional determination of the internal quality of mango requires a destructive methodology using specialised equipment, procedures and trained personnel, which results in high analysis costs and does not allow

62 the whole production to be analysed (Torres *et al.*, 2013). Nevertheless, new
63 technologies to monitor fruit quality changes during the postharvest handling
64 chain are rapidly being introduced, especially those based on non-destructive
65 assessment methods, recently reviewed by Jha *et al.* (2010) and Nicolaï *et al.*
66 (2014). These fast and non-destructive methods can help to provide decisive
67 parameters with which to obtain better quality mango products and to promote
68 consumption of mangoes with better health benefits (Ibarra-Garza *et al.*, 2015).
69 Several non-destructive technologies have been widely explored to predict the
70 quality and maturity of mango, such as nuclear magnetic resonance (NMR) (Gil
71 *et al.*, 2000), impact response (Padda *et al.*, 2011; Wanitchang *et al.*, 2011),
72 electronic nose (Lebrun *et al.*, 2008; Zakaria *et al.*, 2012), hyperspectral
73 analysis (Vélez-Rivera *et al.*, 2014a), and near-infrared spectroscopy
74 (Saranwong *et al.*, 2004). Conversely, some authors, such as Jha *et al.* (2005),
75 have included in their studies the full visible spectrum using spectroscopy in
76 intact mangoes, although studies using colour coordinates are more common,
77 such as Jha *et al.* (2007), Subedi *et al.* (2007) or Rungpichayapichet *et al.*
78 (2015).
79 Schmilovitch *et al.* (2000) studied the feasibility of near-infrared spectroscopy
80 (NIRS) to determine the total soluble solids, firmness and acidity of mangoes
81 cv. 'Tommy Atkins' in relation to the maturity stage. Nagle *et al.* (2010)
82 developed a method to measure total soluble solids, total acidity and dry matter
83 in mango cv. 'Chok Anan' on the trees using NIRS. Theanjumpol *et al.* (2013)
84 studied the possibility of predicting six main chemical substances found in
85 mango fruit cv. 'Keitt' and cv. 'Nam Dok Mai Si Thong', which are important in
86 Thailand, such as glucose, sucrose, citric acid, malic acid, starch and cellulose.

87 They used VIS/NIR spectrometry but decided not to use the visible information
88 to avoid the influence of colour pigments. Jha *et al.* (2013) studied the
89 properties of different mangoes that are important for the Indian production
90 using NIRS in the 1200–2200 nm range to measure properties that make it
91 possible to predict the maturity stage. They were able to predict the sweetness
92 of the mangoes from measurements of total soluble solids and pH (Jha *et al.*,
93 2012) or to determine a maturity index based on the estimations of total soluble
94 solids, dry matter and total acidity that was compared with destructive analysis
95 and sensory panels, and corrected using a constant that depended on the
96 cultivar (Jha *et al.*, 2014). Watanawan *et al.* (2014) studied the 700–1100 nm
97 region in an attempt to correlate total soluble solids, total acidity and dry matter
98 of mango cv. 'Namdokmai' with maturity in order to predict the optimum
99 harvesting time. They found good correlations among NIRS values and
100 firmness and dry matter content at harvest, and predicted TSS with very high
101 accuracy, although they consider that their study needs to be revised in order to
102 reduce the heterogeneity in fruit maturity and increase the outturn quality.
103 The main problem of using NIRS to assess fruit quality is the robustness of the
104 calibration model (Rungpichayapichet *et al.*, 2016). Additionally, fruit cultivar,
105 size, and harvest season also play an important role in the robustness of NIRS
106 models (Bobelyn *et al.*, 2010). In this study, a non-destructive method based on
107 visible and near-infrared spectroscopy was investigated to determine the
108 internal quality of mango cv. 'Osteen' during ripening because this is the main
109 variety of mango grown in Spain. This variety could be included in the group of
110 late-ripening mangoes, with higher weights and prices than other varieties of the
111 same fruit. For this reason, this variety is considered to be optimal for export

112 owing to its late maturing characteristics and final relatively low weight loss
113 (Siller-Cepeda *et al.*, 2009).
114 Hence, the aims of this research were (a) to determine an internal quality index
115 for mangoes, based on their main biochemical (total soluble solids) and physical
116 properties (firmness and flesh colour), avoiding the titratable acidity analysis,
117 because it is a laborious and slow analysis that generates waste, (b) to apply it
118 to mango cv. 'Osteen', and (c) to develop statistical models based on Partial
119 Least Squares (PLS) to predict the internal quality of the samples through the
120 analysis of external VIS-NIR spectral data.
121

122 ## 2. MATERIALS AND METHODS

123 ### 2.1. Experimental procedure

124 A batch of 140 unripe mangoes (*Mangifera indica* L., cv 'Osteen') were obtained
125 from plantations in Málaga (Spain). The fruit selected were free of external
126 damage or diseases, showing a uniform shape and size. All mangoes were
127 washed and dried to completely remove any water from the surface and then
128 were marked on each side. All sets were ripened in a storage chamber at 18.0 ±
129 2.1 ºC and 67.6 ± 3.3% RH. Sets of twenty mangoes were randomly collected
130 and analysed every two-three days until reaching senescence (sixteen days).
131 The visible and near-infrared spectra of the external skin of each mango were
132 measured on the centre of one cheek and two points on the other cheek (Figure
133 1) on each day of storage. After the measurements, the physical and
134 biochemical properties were analysed.

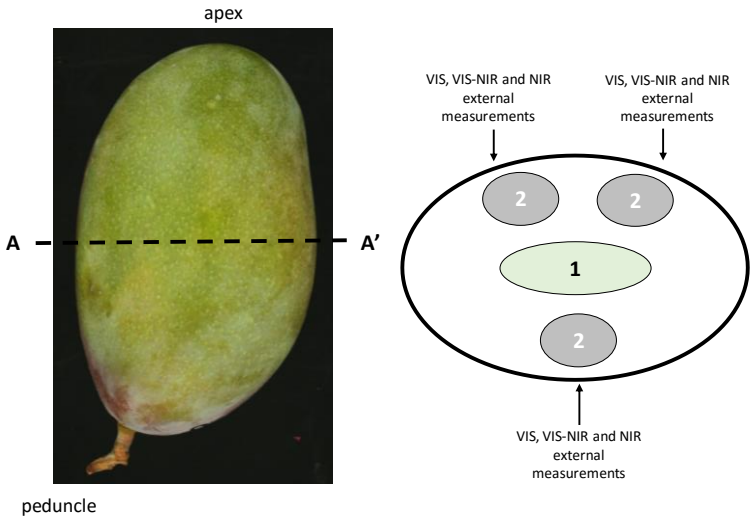

Figure 1. External reflection spectroscopy measurements in fruit slice AA' (1: seed; 2: penetrometer firmness and flesh colour measurement locations).

2.2. Visible and near-infrared spectra collection

The spectral characteristics of the external skin of the intact mangoes were measured in the visible and in the short and medium near-infrared range using a conventional spectrocolorimeter and a VIS-NIR spectrometer.

The external visible spectra of mango samples between 400 and 700 nm, every 10 nm, were measured using a spectrocolorimeter (CM-700d, Minolta Co., Tokyo, Japan). All the measurements were performed by placing the spectrocolorimeter directly onto the skin of the fruit.

The visible-near infrared and near-infrared spectra of mango samples were collected alternately in reflectance mode using a multichannel spectrometer platform (AVS-DESKTOP-USB2, Avantes BV, The Netherlands) equipped with two detectors (Figure 2). The first detector (AvaSpec-ULS2048 StarLine, Avantes BV, The Netherlands) included a 2048-pixel charge-coupled device (CCD) sensor (SONY ILX554, SONY Corp., Japan), 50 µm entrance slit and a

600 lines/mm diffraction grating covering the VIS-NIR range from 600 nm to 1100 nm with a spectral FWHM (full width at half maximum) resolution of 1.15 nm. The spectral sampling interval was 0.255 nm. The second detector (AvaSpec-NIR256-1.7 NIRLine, Avantes BV, The Netherlands) was equipped with a 256 pixel non-cooled InGaAs (Indium Gallium Arsenide) sensor (Hamamatsu 92xx, Hamamatsu Photonics K.K., Japan), a 100 µm entrance slit and a 200 lines/mm diffraction grating covering the NIR range of 900 nm to 1750 nm and a spectral FWHM resolution of 12 nm. The spectral sampling interval was 3.535 nm. A Y-shaped fibre-optic reflectance probe (FCR-7IR200-2-45-ME, Avantes BV, The Netherlands) was configured with an illumination leg which connects the fibre coupled to a stabilised 10 W tungsten halogen light source (AvaLight-HAL-S, Avantes BV, The Netherlands). The light source ensures a permanent light intensity over the whole measurement range. A holder was used to position the sample properly over the probe and the reflectance probe delivered the light to the sample and collected the reflectance from the sample, which was carried by the fibre cable to the spectrometer in use. The reflectance probe, consisting of seven fibres with a diameter of 200 µm, delivered the light to the sample through a bundle of six fibres. The probe tip was designed to provide reflectance measurements at an angle of 45° so as to minimise specular reflectance from the surface of the fruit. The calibration was performed using a 99% reflective white reference tile (WS-2, Avantes BV, The Netherlands) so that the maximum reflectance value over the range of wavelengths was around 90% of saturation.

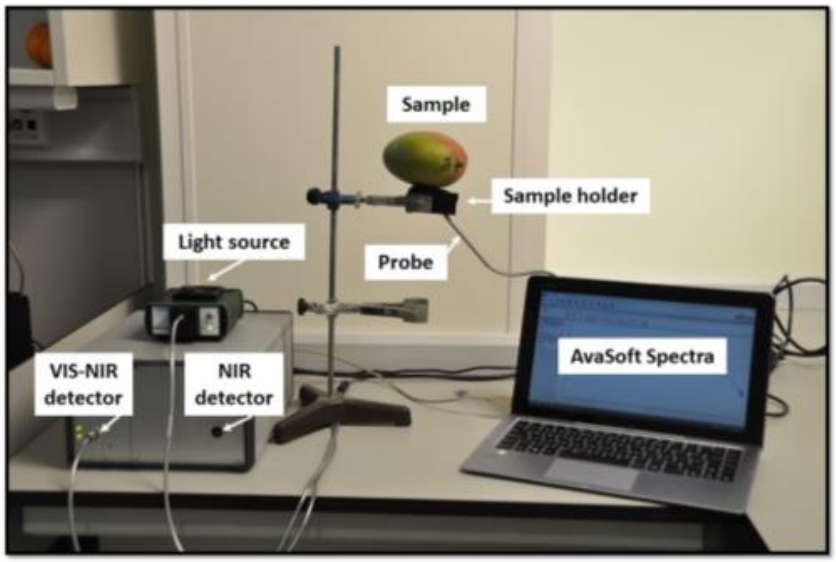

Figure 2. A labelled photograph of the VIS-NIR equipment.

Prior to spectral measurements, the temperature of the mangoes was stabilised at 24 ± 1 °C. Measurements were taken at three longitudinal points over the surface of the fruit and mean values of the spectra were used for the analysis. A personal computer equipped with commercial software (AvaSoft version 7.2, Avantes, Inc.) was used to control both detectors and to acquire the spectra. The signals were pre-processed using AvaSoft software. The integration time was set to 90 ms for the detector sensitive in the VIS-NIR region and to 700 ms for the detector sensitive in the NIR region. For both detectors, each spectrum was obtained as the average of five scans to reduce the thermal noise of the detector (Nicolaï *et al.*, 2007). The average reflectance measurements of each sample (S) were then converted into relative reflectance values (R) with respect to the white reference using dark reflectance values (D) and the reflectance values of the white reference (W), as shown in equation (1):

$$R = \frac{S-D}{W-D} \quad (1)$$

193 The dark spectrum was obtained by turning off the light source and completely
194 covering the tip of the reflectance probe.
195
196 **2.3 Physical and biochemical analysis**
197 The physical properties analysed were firmness, peel colour and flesh colour of
198 the mangoes. The firmness, in Newtons, was analysed through a puncture test
199 by using a universal test machine (TextureAnalyser-XT2, Stable MicroSystems
200 (SMS) Haslemere, England). The tests were performed in triplicate in the axial
201 direction at three locations in the equatorial section (Figure 1 (b)) with a punch
202 with a diameter of 6 mm (P/15ANAMEsignature) until a relative deformation of
203 30%, at a speed of 1 mm/s.
204 CIE (Internationale de l'éclairage) colour values of Luminosity (L^*), chromaticity
205 (C_{ab}^*) and hue angle (h_{ab}^*) for each fruit on both peel (external colour) and flesh
206 (internal colour) were determined using the spectrocolorimeter. The standard
207 illuminant D65 and the 10º standard observer were used for all colour
208 measurements in the study. The colour values were averaged from three
209 different measurements taken at three points on the fruit in order to have
210 representative values. The biochemical properties analysed were the total
211 soluble solids (TSS) and the titratable acidity (TA). TSS content was determined
212 by refractometry with a digital refractometer (set RFM330+, VWR International
213 Eurolab S.L., Barcelona, Spain) at 20 °C and was determined based on the
214 percentage of soluble solids. The analysis of TA was performed with an
215 automatic titrator (CRISON, pH-burette 24, Barcelona, Spain) with 0.5 N NaOH
216 until a pH of 8.1 (UNE34211:1981), using 15 g of crushed mango which was

diluted in 60 mL of distilled water. The TA was determined based on the percentage of citric acid that was calculated using equation 2.

$$Titrable\ acidity[g\ citric\ acid/100\ g\ of sample] = \frac{(A \times B \times C/D) \times 100)}{E} \quad (2)$$

where A is the volume of NaOH consumed in the titration (in L), B is the normality of NaOH (0.5 N), C is the molecular weight of citric acid (192.1g·mol^{-1}), D is the weight of the sample (15 g) and E is the valence of citric acid (E = 3).

Two indices, a ripening index (RPI) and an internal quality index (IQI) were calculated by equations 3 and 4. The RPI was described previously by Vásquez-Caicedo *et al.* (2005) and Vélez-Rivera *et al.* (2014b). However, titratable acidity analysis is complex, laborious, slow and generates waste. Furthermore, the colour has previously been proved to be a quality indicator of mango (Jha *et al.*, 2006a and 2006b). In Jha *et al.* (2007) colour parameters were highly correlated with TSS through the creation of several models based on the CIEL*a*b* coordinates. From these studies, the IQI was calculated combining TSS, firmness, and flesh colour. These parameters have been used in packing houses to measure the quality of mangoes. They require less time, less pre-treatment of the sample and lower costs.

$$RPI = ln(100 \cdot F \cdot TA \cdot TSS^{-1}) \quad (3)$$

$$IQI = ln\left(100 \cdot F \cdot L^{*} \cdot {h_{ab}}^{*} \cdot TSS^{-1} \cdot {C_{ab}}^{*-1}\right) \quad (4)$$

where F is firmness (Newtons), TA is titratable acidity (%), TSS is total soluble solids (%) and L^*, h_{ab}^* and C_{ab}^* are the colour attributes of the flesh colour.

2.4. Statistical Analysis

The spectroscopic data and both indices were organised into three different matrices: the first matrix for the visible spectra (400-700 nm), the second matrix for the VIS-NIR spectra (600-1100 nm) and the third matrix for the NIR spectra (900-1750 nm). In all the matrices, the rows represent the number of samples (#N = 140 samples) and the columns represent the number of variables (X-variables and Y-variables). The X-variables, or predictors, were the different spectra and the Y-variables, or responses, were the two variables provided by RPI and IQI. All the matrices were analysed using The Unscrambler Version 9.7 software package (CAMO Software AS, Oslo, Norway). First, all the spectral data were pre-processed. The X-variables were transformed to apparent absorbance (log (1/R)) values to obtain linear correlations of the NIR values with the concentration of the estimated constituents (Shao *et al.*, 2007; Liu *et al.*, 2010) and centred by subtracting their averages in order to ensure that all results will be interpretable in terms of variation around the mean. Due to the high resolution causing an increased occurrence of signal noise by its spectral range measurement, the VIS-NIR spectra were reduced using a reduction factor of 7. In order to reduce the influence of light scattering (Santos *et al.*, 2013) and the baseline drift various pre-processing methods were applied to the spectra. Savitzky-Golay smoothing with a gap of three data points combined with extended multiplicative scatter correction (EMSC) were considered the best results for the VIS-NIR spectra, and those two pre-treatments and second

derivative with Gap-Segment (2.3) were the best results for the NIR spectra. After the pre-processing steps, the X-variables in the matrices were 31, 285 and 242 for the visible spectrum, VIS-NIR spectrum and NIR spectrum, respectively. Secondly, each set was divided randomly into two groups, a calibration set (75% of the samples) and a prediction set (25% of the samples). Partial least squares regression (PLS) was applied to the matrix to construct separate calibration models for each ripening index and each spectrum with segments of 20 objects (Næs *et al.*, 2004) and it was evaluated by means of a cross validation methodology. PLS defines the latent variables (principal components) based on the covariance between the independent and dependent variables, the advantage of PLS regression being its ability to analyse data with many, noisy, collinear, and even incomplete variables in both X and Y (Næs *et al.*, 2004). This technique has usually been used in multivariate calibration in fruit applications (Liu *et al.*, 2010) and allows obtaining the best results when linear relations between spectra and properties of samples exist (Li *et al.*, 2010). Liu *et al.* (2008) used the MLR technique based on the regression of the discrete parts of the spectra and PLS based on the full spectrum; the results of the two techniques in their study appeared to be very similar.

In order to reduce the high dimensionality of the spectral data, to avoid the presence of noise or information that is not related to the quality characteristics of the mango, and to make the PLS models more robust, the most important wavelengths to predict both indices were selected (ElMasry *et al.*, 2007; Talens *et al.*, 2013). For each calibration model, the weighted regression coefficients resulting from the PLS models were used to select the important wavelengths. Regression coefficients show the weight of the contribution of each wavelength

292 to the calibration model and eliminate the spectral regions with less contribution.
293 Standardised spectral data were used to develop the PLS models to obtain the
294 weighted regression coefficients.
295 The relative performance of the constructed models was assessed by the
296 required number of latent variables (LVs), the coefficient of determination for
297 calibration (R_C^2), the root mean square error of calibration (RMSEC) and the
298 root mean square error of leave-one-out cross-validation (RMSECV). A model
299 can be considered good when a low number of LVs are required and it has a
300 low RMSEC and RMSECV and high R_C^2. The predictive ability of the models
301 was evaluated using the coefficient of determination for prediction (R_P^2), the
302 root mean square error of prediction (RMSEP) and the ratio of prediction to
303 deviation (RPD=SD/RMSEP), where the SD was the standard deviation of the
304 Y-variable in the prediction set. A value below 1.5 for the RPD indicates that the
305 calibration is not usable. A value between 1.5 and 2.0 for the RPD reveals a
306 possibility to distinguish between high and low values, while a value between
307 2.0 and 2.5 makes approximate quantitative predictions possible. For values
308 between 2.5 and 3.0, and above 3.0, the prediction is considered to be good
309 and excellent, respectively (Williams & Sobering, 1993; Saeys *et al.*, 2005;
310 Cozzolino *et al.*, 2011). R^2_C measured the performance of a multivariate
311 calibration model and can be defined as the following Equations 5 and 6
312 (Yahaya *et al.*, 2015):
313
314 $$RMSEC = \sqrt{\frac{1}{n_C}\sum_{i=1}^{n_C}(\hat{y}_i - y_i)^2} \quad (5)$$
315 $$RMSECV \vee RMSEP = \sqrt{\frac{1}{n_p}\sum_{i=1}^{n_p}(\hat{y}_i - y_i)^2} \quad (6)$$

where:

$\hat{y}_i$ is the predicted value of the ith observation

y_i is the measured value of the ith observation

n_C is the number of observations in the calibration set

n_p is the number of observations in the validated set

3. RESULTS AND DISCUSSION

3.1. Changes in mango quality during ripening

Table 1 shows the range (minimum and maximum values), mean and standard deviation of the quality parameters analysed in the mango samples (#N = 140 samples).

Table 1. Descriptive statistics for the quality parameters analysed in the mango samples.

Mango	TSS (%)	TA (%)	Firmness (N)	*L*ext*	*C* ext*	*h*ext*	*L* Int*	*C*int*	*h* Int*
Min	5.8	0.07	11.8	32.0	34.5	14.0	56.3	8.6	70.4
MAX	20.7	0.98	124.3	56.5	65.0	94.2	81.8	46.8	86.1
Mean	13.4	0.47	76.1	43.1	53.0	47.2	72.7	25.2	78.7
Sdev	3.5	0.22	35.8	4.7	6.3	18.3	6.4	9.1	4.0

The firmness ranged from 124.3 to 11.8 N. The peel luminosity, peel chroma and peel hue ranged from 32, 34.5, 14 to 56.5, 65, 94.2, respectively, whereas flesh luminosity, flesh chroma and flesh hue ranged from 56.3, 8.6, 70.4 to 81.8, 46.8 and 86.1, respectively. The TSS and the TA ranged from 5.85 to 19.50% and 0.97 to 0.07%, respectively. Similar values were observed by other authors during the ripening process of mangoes, working with other mango varieties such as ‘Alphonso’ (Yashoda *et al.*, 2007), ‘Tommy Atkins’ (Lucena *et al.*, 2007), ‘Nam Dokmai’ and ‘Irwin’ (Fukuda *et al.*, 2014).

Table 2 shows the Pearson correlation coefficients and was calculated to check for significant inter-correlations between the parameters analysed in mango samples. The results indicated that, in general, peel/external colour showed lower correlations with respect to the other physical and biochemical properties, whereas higher correlations were found between firmness, flesh/internal colour and the biochemical properties. Positive correlations were found between firmness and internal L^* (0.93), internal h_{ab}^* (0.88) and TA (0.63), and negative correlations were found between firmness and internal C_{ab}^* (-0.78) and TSS (-0.79).

Table 2. Pearson correlation coefficients between quality parameters analysed in mango samples.

	TSS (%)	*TA (%)*	*Firmness N*	*L* ext*	*C* ext*	*h* ext*	*L* Int*	*C* int*	*h* Int*	RPI	IQI
TSS (%)	1										
TA (%)	-0.36	1									
Firmness (N)	-0.79	0.63	1								
L*ext	0.16	-0.10	-0.23	1							
C* ext	0.64	-0.52	-0.78	0.15	1						
h*ext	-0.06	0.20	0.08	0.62	-0.21	1					
L* Int	-0.83	0.55	0.93	-0.22	-0.77	0.09	1				
C*int	0.67	-0.59	-0.75	0.46	0.58	0.15	-0.72	1			
h* Int	-0.81	0.54	0.88	-0.16	-0.84	0.22	0.94	-0.67	1		
RPI	-0.76	0.82	0.92	-0.19	-0.72	0.12	0.89	-0.77	0.83	1	
IQI	-0.87	0.63	0.95	-0.29	-0.75	0.02	0.94	-0.87	0.89	0.94	1

Figure 3 shows the changes in firmness, peel and flesh colour, TA and TSS of mangoes at different days of storage. As expected, firmness values of 'Osteen'

354 mangoes decrease constantly during ripening. At the beginning of the process,
355 the firmness remained fairly constant, although a pronounced decrease in the
356 firmness values was observed from eleven to sixteen days of storage, the loss
357 of firmness on the last day of storage being around 75% of the firmness
358 recorded at the beginning of the study. A similar behaviour has been reported
359 for other mango varieties such as ‘Alphonso’ (Yashoda *et al.*, 2005), ‘Ataulfo’
360 (Palafox-Carlos *et al.*, 2012) or ‘Keitt’ (Ibarra-Garza *et al.*, 2015). These
361 changes can be attributed to different factors, such as the enzymatic activity
362 (Prasanna *et al.*, 2007; Yashoda *et al.*, 2007) and/or the solubilisation, de-
363 esterification, and de-polymerisation of the middle lamella, accompanied by an
364 extensive loss of neutral sugars and galacturonic acid (Singh *et al.*, 2013),
365 which modify the structural integrity of the cell wall and middle lamella.
366

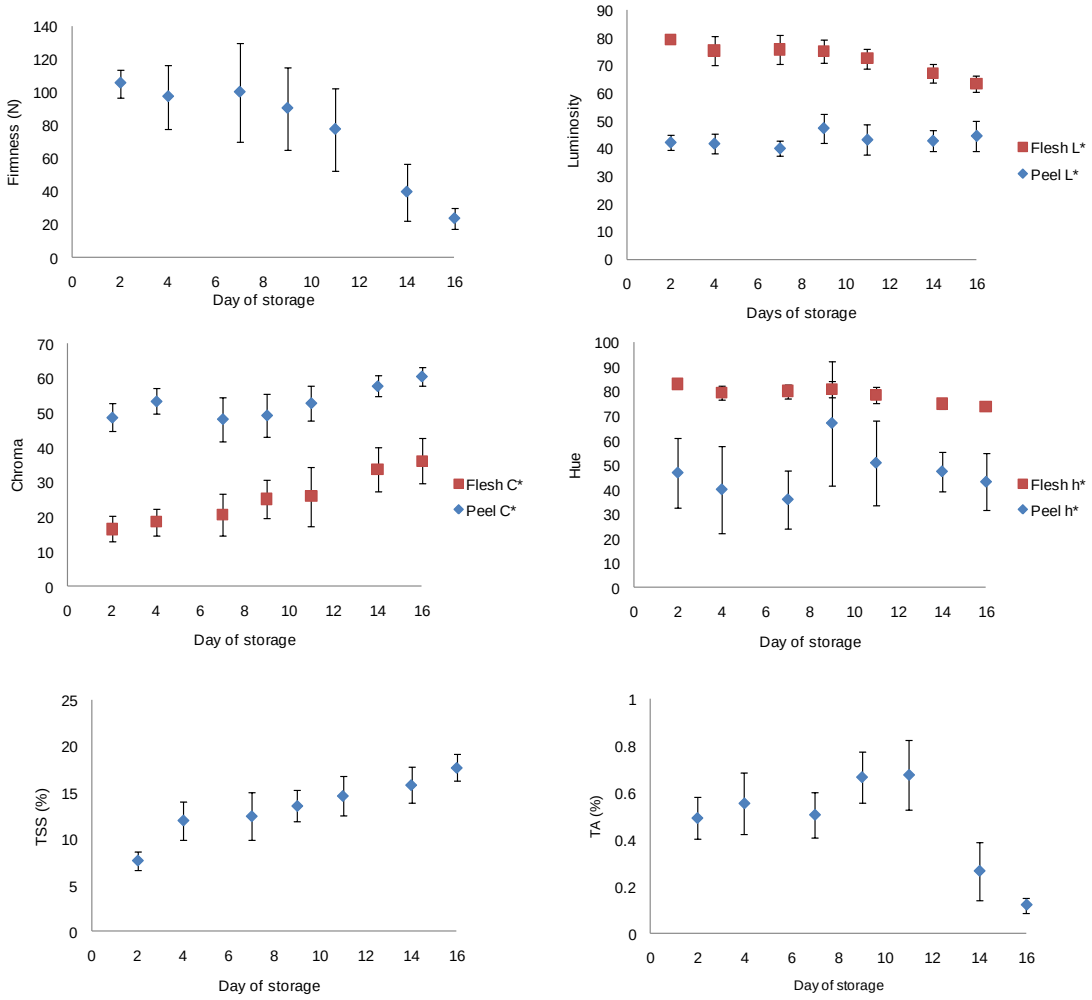

Figure 3. Mean and standard deviation of firmness, peel colour, flesh colour, TSS and TA of mangoes at different days of analysis.

The changes in peel/external and flesh/internal colour observed during the ripening of mangoes cv. 'Osteen' are also shown in Figures 3 and 4. Whereas flesh luminosity and flesh hue values decreased from 79º to 63º and from 83º to 74º, respectively, and flesh chroma values increased from 16 to 36, no clear changes in peel luminosity and peel hue values and small differences in peel chroma values could be observed, which is logical since the colour of the peel is heterogeneous and varies from one sample to another. In general, the peel colour changes were not uniform, indicating that peel colour is not an adequate quality parameter for cv. 'Osteen' mango cultivars.

However, flesh colour changes were uniform when fruit advances in ripening and can serve as an adequate quality parameter (Figures 3 and 4). The increase in the yellow-orange intensity of mango flesh can be associated with an increase in carotenoid content of mango fruit, as has been reported previously by other authors (Ornelas-Paz *et al.*, 2008; Ibarra-Garza *et al.*, 2015). This change is accompanied by a decrease in the *L** value, although, despite the correlation, there is no evidence that the changes in the luminosity of the flesh (*L**) are actually due to the increase in carotenoids.

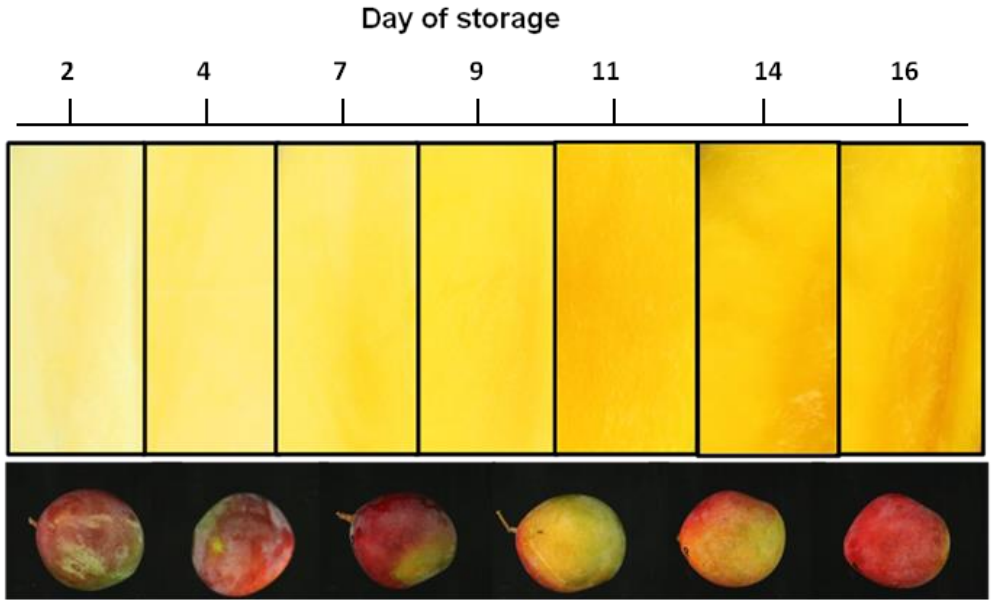

Figure 4. External appearance and flesh colour of mango cv. 'Osteen' at different days of storage.

Loss of firmness and changes in flesh colour correlate with the increase of the TSS ratio and decrease of TA (Figure 3). During ripening the TSS increased due to the conversion of starch into glucose and fructose, which are used as substrates during fruit respiration (Eskin *et al.*, 2013), while the TA tends to

decrease due to the cell metabolisation of volatile organic acids and non-volatile constituents (Padda *et al.*, 2011).

Taking into account the strong correlation found between the biochemical properties (TSS and TA) and the firmness and flesh colour (Table 2), two indices were calculated. The ripening index, RPI, involves the most essential physical and biochemical properties of the fruit linked with the sensory perception of the ripeness of the mangoes. The internal quality index, IQI, was calculated because it is a good indicator to assess changes in the mesocarp during the ripening of mangoes. In fact, firmness, total soluble solids and flesh/internal colour are the three parameters used in mango packing-lines to assess mango quality and stage of ripeness (Brecht *et al.*, 2010), whereas the TA is more difficult and laborious to determine. Table 2 shows the Pearson correlation coefficient between the two indices, with higher positive correlations (0.94). Figure 4 shows the changes in the RPI and IQI indices calculated for the mangoes at different days of storage. In both cases, it can be observed that the values of the indices decreased during ripening. Based on previous studies working with RPI in mango cv. 'Manila' (Vélez-Rivera *et al.*, 2014b) and comparing the values of this study, three ripeness phases were identified: unripe mangoes (values higher than 6, day two), intermediate-ripe mangoes (values between 6 and 4, days four to eleven) and over-ripe mangoes (values less than 4, days fourteen to sixteen), the intermediate-ripe mangoes being the mangoes with the best quality.

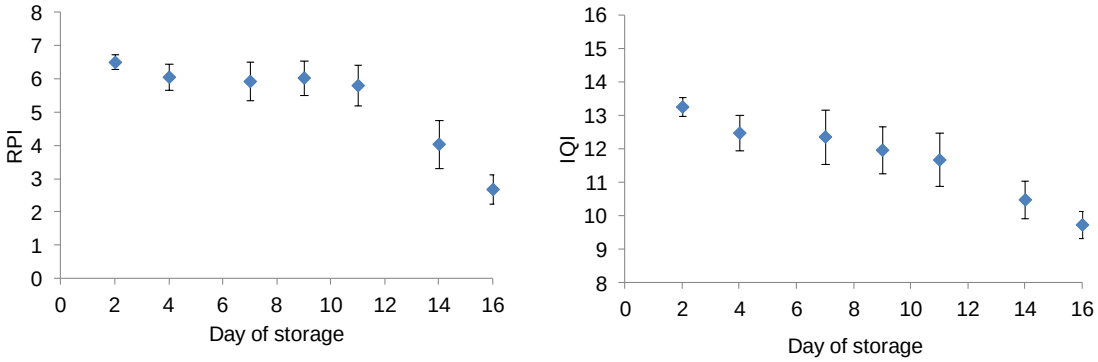

Figure 5. RPI and IQI of mangoes at different days of storage.

3.2. Analysis of visible and near-infrared spectra

When assessing ripening with a visible and/or near-infrared spectroscope, it is crucial to identify the spectral changes associated with pigment evolution and compositional changes. Typical apparent absorbance spectral of mangoes at different ripening stages for the visible region, the VIS-NIR and the NIR regions are shown in Figure 6.

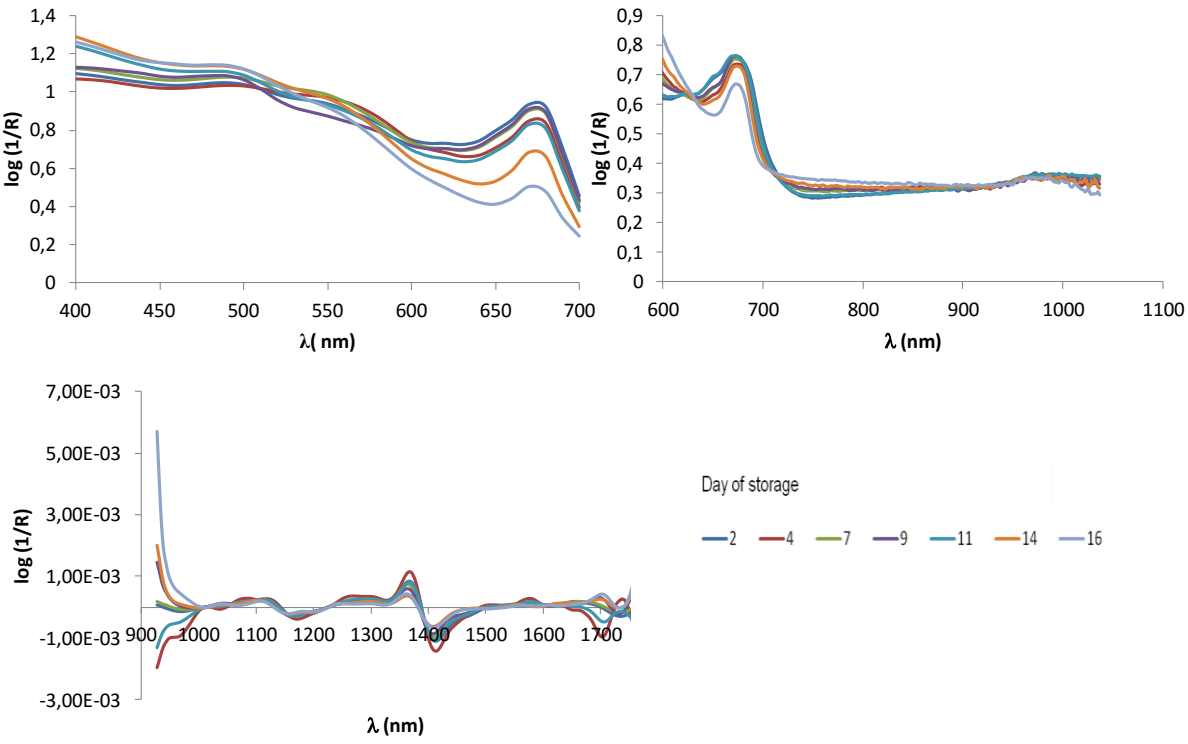

Figure 6. Apparent absorbance spectra of mangoes at different ripening stages for the (a) visible region, (b) the VIS-NIR region and (c) the NIR region after pre-treatments.

All the spectra have a similar pattern with the main maxima located in the visible and near-infrared region, which showed the strong absorbance characteristics of the mangoes within the range of study. In the visible range, the light peaks around 400-500 nm are correlated with the carotenoid pigments (Lichtenthaler & Buschmann, 2001) and the peak around 640-700 nm illustrated the colour transition of mangoes correlated with the chlorophyll content that absorbs radiation in this region (Merzlyak *et al.*, 2003). Similarly, Knee (1980) and Bodria *et al.* (2004) analysed apples and claimed that their reflectance minimum in the 670 nm to 680 nm range was strongly related to chlorophyll content. Therefore, the ripening process of the fruit, with changes in chlorophyll, carotenoid and anthocyanin contents, indicated the influence of pigment content and composition on the colouration of the entire spectral visible reflectance of the fruit (Yahaya *et al.*, 2014; Omar, 2013). This view is supported by the study of Magwaza *et al.* (2012), who described the pattern of the absorption curves for Satsuma mandarin, which is similar to that for other fruit like mangoes and kiwis. On the other hand, the water peaks were recorded at around 950-1050 nm and 1350-1550 nm due to the second overtone of the OH stretching band (Büning-Pfaue, 2003), and the variations at 1100-1250 nm are correlated with the sugar content (Osborne *et al.*, 1993; Walsh *et al.*, 2004). Figure 5a and 5b shows an increase in absorbance within the blue region during ripening, mainly linked to an increase in the carotenoids content, and a decreased

absorbance in the red region, mainly linked to a decrease in the chlorophyll content. Merzlyak *et al.* (2003) suggested that carotenoid synthesis is induced when chlorophyll degradation occurs during fruit ripening and senescence. Also during ripening, an increase in TSS is produced and could be mainly due to hydrolysis of starch into soluble sugars such as sucrose, glucose and fructose (Agravante *et al.*, 1990; Cordenunsi & Lajolo, 1995).

3.3. Non-destructive prediction of mango quality

Multivariate analysis was performed in order to establish the quantitative relationship between the absorbance spectra and the internal quality of mango. The full range spectra for the three regions studied were used to establish calibration models based on PLS to explain RPI and IQI. The performance of the calibration models was optimised by internal cross-validation and then validated by external validation in an independent validation set.

Table 3 and Table 4 show the results obtained for the calibration and cross-validation sets for the three models developed. Similar results on the calibration and cross-validation sets were obtained to predict RPI and IQI using the VIS, VIS-NIR or NIR detector. The models were very accurate with high R_C^2 (0.902-0.934) and R_{CV}^2 (0.831-0.903), while RMSEC (0.335-0.509) and RMSECV (0.395-0.546) were low. The models applied to the independent validation set were capable of predicting RPI with R_P^2 of 0.871, 0.902 and 0.845, and RMSEP of 0.520, 0.470 and 0.592, respectively, for the three spectral regions. On the other hand, the results achieved for the IQI were R_P^2 of 0.879, 0.877 and 0.833, and RMSEP of 0.464, 0.435 and 0.507, respectively, for the VIS, VIS-NIR and NIR detector. Although better results were obtained when visible information

was used, the models developed using the VIS/NIR and NIR spectra also presented high values of R_P^2 and low values of RMSEP.

Table 3. Results of the PLS models for the calibration and prediction of RPI in mango samples by using the full spectral range and the important wavelengths.

			CALIBRATION		CROSS VALIDATION		PREDICTION		
DETECTOR	**#W**	**#LV**	**R_C^2**	**RMSEC**	**R_{CV}^2**	**RMSECV**	**R_P^2**	**RMSEP**	**RPD**
VIS	31	6	0.907	0.415	0.886	0.463	0.871	0.520	2.916
	5	4	0.893	0.445	0.882	0.471	0.871	0.520	2.827
VIS-NIR	285	8	0.934	0.335	0.902	0.412	0.902	0.470	2.767
	6	6	0.847	0.509	0.827	0.546	0.795	0.548	2.373
NIR	242	10	0.922	0.364	0.868	0.478	0.845	0.592	2.340
	9	5	0.853	0.499	0.830	0.542	0.831	0.613	2.259

Table 4. Results of the PLS models for the calibration and prediction of IQI in mango samples by using the full spectral range and the important wavelengths.

			CALIBRATION		CROSS VALIDATION		PREDICTION		
DETECTOR	**#W**	**#LV**	**R_C^2**	**RMSEC**	**R_{CV}^2**	**RMSECV**	**R_P^2**	**RMSEP**	**RPD**
VIS	31	6	0.916	0.363	0.903	0.395	0.879	0.464	2.826
	5	4	0.881	0.433	0.871	0.455	0.838	0.537	2.522
VIS-NIR	285	4	0.905	0.389	0.891	0.421	0.877	0.435	2.691
	5	5	0.827	0.525	0.796	0.575	0.896	0.403	2.905
NIR	242	10	0.902	0.394	0.831	0.523	0.833	0.507	2.341
	7	5	0.841	0.503	0.820	0.540	0.815	0.531	2.060

The RPD values of the resulting models gave the relative predictive performance of the model more directly in comparison to either R^2 or RMSEP used alone. In this study, the RPD values obtained were 2.916, 2.767 and 2.340 for RPI and 2.826, 2.691 and 2.341 for IQI for the VIS, VIS-NIR and NIR detectors, respectively. In all cases they are high values indicating a greater ability of the models to accurately predict the internal ripeness of the mango in new samples.

Figure 7 shows the regression coefficient plots with the important wavelengths for RPI and IQI for each spectral range. These wavelengths corresponded to -H and -OH functional groups, which are related to carbohydrates (namely sugars and starches), organic acids and water (Rungpichayapichet *et al.*, 2016).

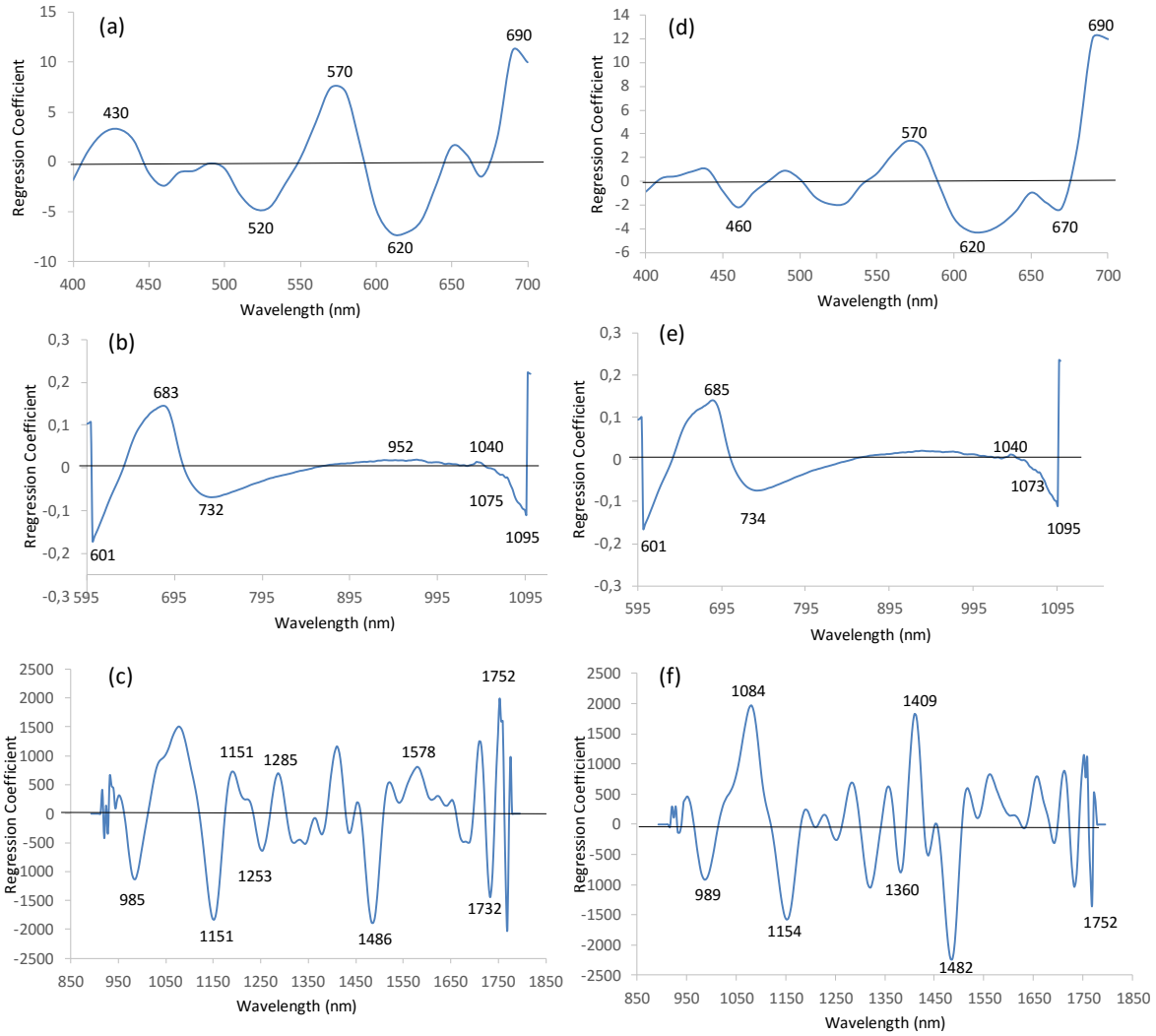

Figure 7. Regression coefficient plot of PLS calibration models developed from overall data for RPI (a, b and c) and IQI (d, e and f) for each spectral range.

After identifying the optimal wavelengths, the reduced sets of bands were used to build new PLS models using the absorbance at these particular wavelengths as independent variables, and the measured values of RPI and IQI as dependent variables. Figure 8 shows the efficiency of PLS models for this

prediction, indicating that it is possible to use a reduced number of bands in the visible and near-infrared region to predict the internal quality of mango 'Osteen'.

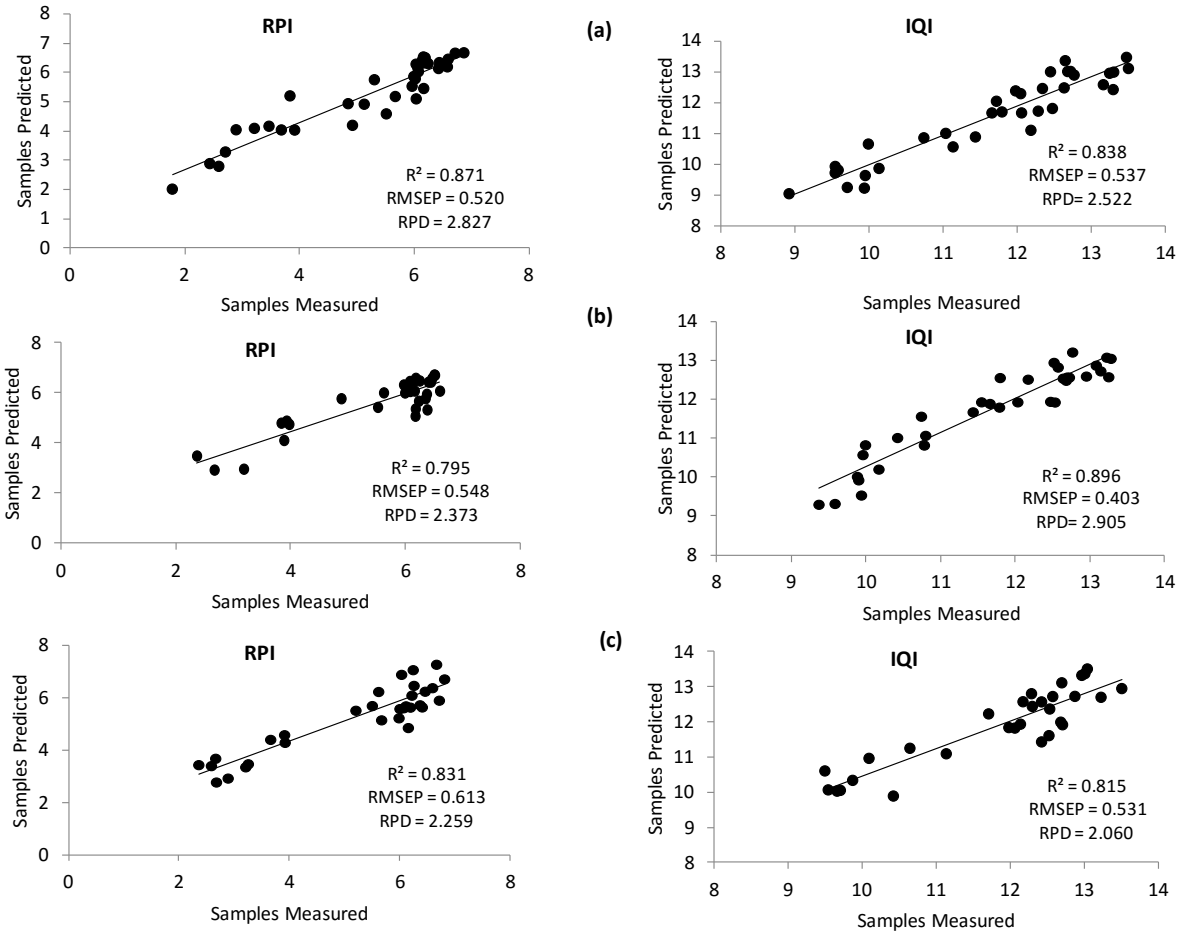

Figure 8. Predicted versus measured values of RPI and IQI for the visible region (a), the visible-near infrared region (b) and near-infrared region (c).

The feasibility of VIS-NIR to predict RPI of mango was indicated by an R_p^2 between 0.795-0.871, RMSEP of 0.520-.613 and RPD of 2.259-2.827 (Figure 8). The results corroborated other studies on the use of spectroscopy techniques to predict RPI, such as Mahayothee (2005), with R^2 of 0.8 and SEP of 0.9, or Rungpichayapichet *et al.* (2016) with $R^2 > 0.8$ and SEP > 0.8 for 'Nam Dokmai' mangoes. Other indices that have been developed, for example, Jha *et al.* (2007), predicted the maturity index (I_m) using colour values with a

correlation of 0.92 and SEP of 10.72 for mango cv. Dashehari. Likewise, IQI has been identified as a quality indicator for mango cv. 'Osteen', and in this study R_p^2, RMSEP and RPD values were between 0.815-0.896, 0.403-0.537 and 2.060-2.905 respectively. As shown in Table 3 and Table 4, the PLS models created from the selected wavelengths reduced the number of latent variables while maintaining a similar performance to PLS models created with the full spectrum. Likewise, their calibration and prediction errors do not worsen and both indices remain the same range in mango samples.

4. CONCLUSIONS

The internal quality of intact mango 'Osteen' fruit has been assessed using external visible and near-infrared reflection spectroscopy. In order to assess the internal quality of the fruit, two indices have been used, the ripening index (RPI) and the internal quality index (IQI). Different spectroscopy systems were used to measure different spectral ranges (VIS, VIS-NIR and NIR) externally in reflectance mode. The partial least squares regression analysis showed a strong performance in predicting RPI and IQI for the VIS, VIS-NIR and NIR detectors using the full spectral range and the most important wavelengths. However, accuracy may be compromised when the measuring is being implemented on samples with different external geometry by two spectroscopy systems that are structured differently in terms of their optical-electronics configuration within the spectrometer or in their interfacing with the sample. Nevertheless, the results obtained from this study clearly reveal that external visible and near-infrared spectroscopy combined with chemometrics can be used for the non-destructive prediction of the internal quality of mango 'Osteen'.

This technological development could even be integrated in continuous fruit packing lines as part of the quality assurance system.

5. Acknowledgements

This work was partially funded by the Conselleria d' Educació, Investigació, Cultura i Esport, Generalitat Valenciana, through the project AICO/2015/122 and by the INIA through the projects RTA2012-00062-C04-01, 02 and 03 with the support of FEDER funds. V. Cortés López thanks the Spanish MEC for the FPU grant (FPU13/04202).

6. References

AENOR, 1981. Productos derivados de frutas y verduras, determinación de la acidez valorable. UNE 34211:1981.

Agravante, J.U., Matsui, T. & Kitagawa, H. (1990). Starch breakdown in ethylene and ethanol treated bananas: changes in phosphorylase and invertase activities during ripening. J. Jpn. Soc. Food Sci., 37, 911-915.

Bobelyn, E., Serban, A.S., Nicu, M., Lammertyn, J., Nicolai, B.M. & Saeys, W. (2010). Postharvest quality of apple predicted by NIR-spectroscopy: Study of the effect of biological variability on spectra and model performance. Postharvest Biology and Technology, 55, 133-143.

Bodria, L., Fiala, M., Guidetti, R. & Oberti, R. (2004). Optical techniques to estimates the ripeness of red-pigmented fruits. Transactions of the ASAE, 47, 815.

573 Brecht J., Sargent S., Kader A., Mitcham E., Maul F., Brecht P., & Menocal O.
574 (2010). Mango Postharvest Best Management Practices Manual. *Gainesville:*
575 *Univ.of Fla. Horticultural Sciences Department*, 78.

576 Büning-Pfaue, H. (2003). Analysis of water in food by near infrared
577 spectroscopy. Food Chemistry, 82, 107-115.

578 Cordenunsi, B.R. & Lajolo, F.M. (1995). Starch Breakdown During Banana
579 Ripening: Sucrose Synthase and Sucrose Phosphate Syntase Behavior.
580 Journal Agricultural Food Chemistry, 43, 347-351.

581 Cozzolino, D., Cynkar, W.U., Shah, N. & Smith, P. (2011). Multivariate data
582 analysis applied to spectroscopy: Potential application to juice and fruit
583 quality. *Food Research International,* 44(7), 1888-1896.

584 ElMasry, G., Wang, N., ElSayed, A. & Ngadi, M. (2007). Hyperspectral imaging
585 for nondestructive determination of some quality attributes for strawberry.
586 *Journal of Food Engineering,* 81(1), 98-107.

587 Eskin, N.A.M., Hoehn, E. & Shahidi, F. (2013). Fruits and vegetables.*Eskin,*
588 *N.A.M., Shahidi, F. (Eds.), Biochemistry of foods*, 49–126.

589 Fukuda, S., Yasunaga, E., Nagle, M., Yuge, K., Sardsud, V., Spreer, W. &
590 Müller, J. (2014). Modelling the relationship between peel colour and the
591 quality of fresh mango fruit using Random Forests. *Journal of Food*
592 *Engineering,* 131, 7-17.

593 Galán, S. V. & Farré, M. J. M. (2005). Tropical and Subtropical Fruits in Spain.
594 *ActaHortic.*, 694, 259-264.

595 Gil, A., Duarte, I., Delgadillo, I., Colquhoun, I., Casuscelli, F.,
596 Humpfer,E.&Spraul, M. (2000). Study of the Compositional Changes of

597 Mango during Ripening by Use of Nuclear Magnetic Resonance
598 Spectroscopy. *Journal of Agricultural and Food Chemistry*, *48*(5), 1524-1536.
599 Giovannoni, J.J. (2004). Genetic regulation of fruit development and ripening.
600 *Plant Cell* 16, 170–180.
601 Hernández, Y., Lobo, M.G. & González, M. (2006). Determination of vitamin C
602 in tropical fruits: A comparative evaluation of methods. *Food Chemistry,*
603 96(4), 654-664.
604 Ibarra-Garza, I.P., Ramos-Parra, P.A., Hernández-Brenes, C. & Jacobo-
605 Velázquez, D.A. (2015). Effects of postharvest ripening on the nutraceutical
606 and physicochemical properties of mango (Mangiferaindica L. cv Keitt).
607 *Postharvest Biology and Technology,* 103, 45-54.
608 Jha, S.N., Chopra, S. & Kingsly, A.R.P. (2005). Determination of Sweetness of
609 Intact mango using Visual Spectral Analysis. Biosystems Engineering, 91 (2),
610 157-161.
611 Jha, S. N., Kingsly, A.R.P. & Chopra, S. (2006a). Physical and mechanical
612 properties of mango during growth and storage for determination of maturity.
613 Journal of Food Engineering, 72(1), 73 – 76. 6.
614 Jha, S. N., Kingsly A.R.P. & Chopra S. (2006b). Nondestructive determination
615 of firmness and yellowness of mango during growth and storage using visual
616 spectroscopy. Biosystems Engineering, 94(3), 397 - 402. 7.
617 Jha, S.N., Chopra, S. & Kingsly, A.R.P. (2007). Modeling of color values for
618 nondestructive evaluation of maturity of mango. Journal of Food Engineering,
619 78, 22-26.
620 Jha, S. N., Narsaiah, K., Sharma, A.D., Manpreet, S., Sunil, B. & Kumar, R.
621 (2010). Quality parameters of mango and potential of non-destructive

techniques for their measurement – a Review. Journal of Food Science and Technology, 47(1), 1-14. 4.

Jha, S.N., Jaiswal, P., Narsaiah, K., Singh, A.K., Kaur, P.P., Sharma, R., Kumar, R.& Bhardwaj, R. (2011). Prediction of Sensory Profile of Mango Using Textural Attributes During Ripening. *Food and Bioprocess Technology,* 6, 734-745.

Jha, S.N., Jaiswal, P., Narsaiah, K., Gupta, M., Bhardwaj, R. & Singh, A.K. (2012). Non-destructive prediction of sweetness of intact mango using near infrared spectroscopy. *Scientia Horticulturae,* 138, 171-175.

Jha, S N., Jaiswal P, Narsaiah K, Sharma R, Bhardwaj R, Gupta M, Kumar R. (2013). Authentication of mango varieties using near infrared spectroscopy. Agricultural Research,2(3):229 – 235. 3.

Jha, S.N., Narsaiah, K., Jaiswal, P., Bhardwaj, R., Gupta, M., Kumar, R. & Sharma, R. (2014). Nondestructive prediction of maturity of mango using near infrared spectroscopy. *Journal of Food Engineering,* 124, 152-157.

Kienzle, S., Sruamsiri, P., Carle, R., Sirisakulwat, S., Spreer, W. &Neidhart, S. (2011). Harvest maturity specification for mango fruit (Mangiferaindica L. 'Chok Anan') in regard to long supply chains. *Postharvest Biology and Technology,* 61, 41–55.

Knee, M. (1980). Methods of measuring green colour and chlorophyll content of apple fruit. Journal Food Technology, 15, 493.

Lebrun, M., Plotto, A., Goodner, K., Ducamp, M. & Baldwin, E. (2008). Discrimination of mango fruit maturity by volatiles using the electronic nose and gas chromatography. *Postharvest Biology and Technology,* 48(1), 122-131.

Lichtenthaler, H. K. & Buschmann, C. (2001). Chlorophylls and Carotenoids: Measurement and Characterization by UV-VIS Spectroscopy. *Current Protocols in Food Analytical Chemistry,* F:F4:F4.3.

Liu, Y., Chen, X., Ouyang, A. (2008). Nondestructive determination of per internal quality indices by visible and near-infrared spectrometry. LWT-Food Sci. Technol. 41, 1720–1725.

Liu, Y., Sun, X. & Ouyang, A. (2010). Nondestructive measurement of soluble solid content of navel orange fruit by visible–NIR spectrometric technique with PLSR and PCA-BPNN. *Food Science and Technology,* 43(4), 602-607.

Lucena, E., Simão de Assis, J., Alves, R., Macêdo da Silva, V. & Filho, J. (2007). Alterações físicas e químicas durante o desenvolvimento de mangas 'Tommy Atkins' no vale de São Francisco, Petrolina-PE. *Rev. Bras. Frutic.* [online], 29(1), 96-101.

Magwaza, L.S., Opara, U.L., Nieuwoudt, H., Cronje, P.J.R., Saeys, W. & Nicolaï, B. (2012). NIR Spectroscopy Applications for Internal and External Quality Analysis of Citrus Fruit: a review. Food Bioprocess Technology, 5, 425.

Mahayothee, B. (2005). The influence of raw material on the quality of dried mango slices (Mangifera indica L.) with special reference to postharvest ripening. Ph.D. Thesis, Hohenheim University. In Schriftenreihe des Lehrstuhls Lebensmittel pflanzlicher Herkunft; Carle, R., (Ed.); Shaker Verlag: Aachen, Germany.

Mercadante, A.Z. & Rodriguez-Amaya, D.B. (1998). Effects of Ripening, Cultivar Differences, and Processing on the Carotenoid Composition of Mango. *Journal of Agricultural and Food Chemistry,* 46(1), 128-130.

672 Merzlyak, M.N., Solovchenko, A.E. & Gitelson, A.A. (2003). Reflectance
673 spectral features and non-destructive estimation of chlorophyll, carotenoid
674 and anthocyanin content in apple fruit. *Postharvest Biology and Technology,*
675 27(2), 197-211.
676 Næs, T., Isaksson, T., Fearn, T. & Davies, T. (2004). A User-Friendly Guide to
677 Multivariate Calibration and Classification. *NIR Publications, Charlton,*
678 *Chichester, UK.*
679 Nagle, M., Mahayothee, B., Rungpichayapichet, P., Janjai, S. & Müller, J.
680 (2010). Effect of irrigation on near-infrared (NIR) based prediction of mango
681 maturity. *Scientia Horticulturae,* 125(4), 771-774.
682 Nicolaï, B.M., Beullens, K., Bobelyn, E., Peirs, A., Saeys, W., Theron, I. K. &
683 Lammertyn, J. (2007). Non-destructive measurement of fruit and vegetable
684 quality by means of NIR spectroscopy: a review. Postharvest Biology and
685 Technology, 46, 99-118.
686 Nicolaï, B., Defraeye, T., De Ketelaere, B., Herremans, E., Hertog, M.L.A.T.M.,
687 Saeys,W., Torricelli, A., Vandendriessche, T. & Verboven, P. (2014).
688 Nondestructive measurements of fruit and vegetable quality. *Ann. Rev. Food*
689 *Sci. Technol.,* 5, 285–312.
690 Omar, A.F. (2013). Spectroscopic profiling of soluble solids content and acidity
691 of intact grape, lime and star fruit. Sensor Rev. 33, 238.
692 Ornelas-Paz, J.D.J., Yahia, E.M., Gardea-Bejar, A.A. (2008). Changes in
693 external and internal color during postharvest ripening of ‘Manila’ and
694 ‘Ataulfo’ mango fruit and relationship with carotenoid content determined by
695 liquid chromatography–APcI+-time-of-flight mass spectrometry. *Postharvest*
696 *Biology and Technology,* 50(2), 145-152.

697 Osborne, B.G., Fearn, T. & Hindle, P. H. (1993). Practical NIR Spectroscopy
698 with Applications in Food and Beverage Analysis. 2nd ed., Longman Group,
699 Burnt Mill, Harlow, Essex, England, UK, p. 123-132.
700 Padda, S.M., do Amarante, C.V.T., Garcia, R.M., Slaughter, D.C. & Mitcham,
701 E.M. (2011). Methods to analyze physicochemical changes during mango
702 ripening: a multivariate approach. *Postharvest Biology and Technology*, 62,
703 267–274.
704 Palafox-Carlos, H., Yahia, E., Islas-Osuna, M.A., Gutierrez-Martinez, P.,
705 Robles-Sánchez, M. & González-Aguilar, G.A. (2012). Effect of ripeness
706 stage of mango fruit (Mangiferaindica L., cv. Ataulfo) on physiological
707 parameters and antioxidant activity. *Scientia Horticulturae,* 135(0), 7-13.
708 Prasanna, V., Prabha, T. N. & Tharanathan, R. N. (2007). Fruit Ripening
709 Phenomena- An Overview. *Critical Reviews in Food Science and Nutrition*,
710 47, 1-19.
711 Rungpichayapichet, P., Mahayothee, B., Khuwijitjaru, P., Nagle, M. & Müller, J.
712 (2015). Non-destructive determination of β-carotene content in mango by
713 near-infrared spectroscopy compared with colorimetric measurements.
714 Journal of Food Composition and Analysis, 38, 32-41.
715 Rungpichayapichet, P., Mahayothee, B., Nagle, M., Khuwijitjaru, P. & Müller, J.
716 (2016). Robust NIRS models for non-destructive prediction of postharvest
717 fruit ripeness and quality in mango. Postharvest Biology and Technology,
718 111, 31-40.
719 Saeys, W., Mouazen, A.M. & Ramon, H. (2005). Potential for Onsite and Online
720 Analysis of Pig Manure using Visible and Near Infrared Reflectance
721 Spectroscopy. *Biosystems Engineering,* 91(4), 393-402.

722 Santos, J., Trujillo, L.A., Calero, N., Alfaro, M.C. & Muñoz, J. (2013). Physical
723 characterization of a commercial suspoemulsion as a reference for the
724 development of suspoemulsions. Chem. Eng. Technol. 11, 1–9.
725 Saranwong, S., Sornsrivichai, J. & Kawano, S. (2004). Prediction of ripe-stage
726 eating quality of mango fruit from its harvest quality measured
727 nondestructively by near infrared spectroscopy. Postharvest Biology and
728 Technology, 31, 137-145.
729 Schmilovitch, Z., Mizrach, A., Hoffman, A., Egozi, H. & Fuchs, Y. (2000).
730 Determination of mango physiological indices by near-infrared spectrometry.
731 *Postharvest Biology and Technology,* 19(3), 245-252.
732 Shao, Y., He, Y., Gómez, A.H., Pereir, A.G., Qiu, Z. & Zhang, Y. (2007).
733 Visible/near infrared spectrometric technique for nondestructive assessment
734 of tomato 'Heatwave' (Lycopersicumesculentum) quality characteristics.
735 *Journal of Food Engineering,* 81(4), 672-678.
736 Siller-Cepeda, J., Muy-Rangel, D., Báez-Sañudo, M., Araiza-Lizarde, E. & Ireta-
737 Ojeda, A. (2009). Calidad poscosecha de cultivares de mango de
738 maduración temprana, intermedia y tardía. *Revista Fitotecnia Mexicana,*
739 32(1), 45.
740 Singh Z., Singh R.K., Sane V.A., & Nath P. (2013). Mango – Postharvest
741 Biology and Biotechnology. *Critical Reviews in Plant Sciences*, 32(4), 217-
742 236.
743 Subedi, P. P., Walsh, K. B. & Owens, G. (2007). Prediction of mango eating
744 quality at harvest using short-wave near infrared spectrometry. Postharvest
745 Biology and Technology, 43, 326-334.

746 Talens, P., Mora, L., Morsy, N., Barbin, D.F., ElMasry, G. & Sun, D. (2013).
747 Prediction of water and protein contents and quality classification of Spanish
748 cooked ham using NIR hyperspectral imaging. *Journal of Food Engineering,*
749 117(3), 272-280.
750 Theanjumpol, P., Self, G., Rittiron, R., Pankasemsu, T., & Sardsud, V. (2013).
751 Selecting Variables for Near Infrared Spectroscopy (NIRS) Evaluation of
752 Mango Fruit Quality. *Journal of Agricultural Science,* 5(7).
753 Torres, R., Montes, E.J., Perez, O.A. & Andrade, R.D. (2013). Relacion del
754 color y del estado de madurez con las propiedades fisicoquimicas de frutas
755 tropicales. *Información Tecnológica,* 24(4), 51.
756 Vásquez-Caicedo, A.L., Sruamsiri, P., Carle, R. &Neidhart, S. (2005).
757 Accumulation of all-trans-b-carotene and its 9-cis and 13-cis stereoisomers
758 during postharvest ripening of nine Thai mango cultivars. *Journal of*
759 *Agricultural and Food Chemistry*, 53, 4827–4835.
760 Vélez-Rivera N., Blasco J., Chanona-Pérez J., Calderón-Domínguez G., Perea-
761 Flores M. J., Arzate-Vázquez I., Cubero S. & Farrera-Rebollo R. (2014b).
762 Computer vision system applied to classification of 'Manila' mangoes during
763 ripening process. *Food and Bioprocess Technology*, 7, 1183-1194.
764 Vélez-Rivera, N., Gómez-Sanchis, J., Chanona-Pérez, J., Carrasco, J.J., Millán-
765 Giraldo, M., Lorente, D., Cubero, S. & Blasco, J. (2014a). Early detection of
766 mechanical damage in mango using NIR hyperspectral images and machine
767 learning. *Biosystems Engineering,* 122, 91-98.
768 Walsh, K. B., Golic, M. & Greensill, C. V. (2004). Sorting of fruit and vegetables
769 using near infrared spectroscopy: application to soluble solids and dry matter
770 content. Journal of Near Infrared Spectroscopy, 12, 141–148.

771 Wanitchang, P., Terdwongworakul, A., Wanitchang, J. & Nakawajana, N.
772 (2011). Non-destructive maturity classification of mango based on physical,
773 mechanical and optical properties. *Journal of Food Engineering,* 105(3), 477-
774 484.
775 Watanawan, C., Wasusri, T., Srilaong, V., Wongs-Aree, C. & Kanlayanarat, S.
776 (2014). Near infrared spectroscopic evaluation of fruit maturity and quality of
777 export Thai mango (Mangiferaindica L. var. Namdokmai). *International Food*
778 *Research Journal,* 21(3), 1073-1078.
779 Williams, P. & Sobering, D. (1993). Comparison of commercial near infrared
780 transmittance and reflectance instruments for analysis of whole grains and
781 seeds. Journal of Near Infrared Spectroscopy, 1, 25.
782 Yahaya, O.K.M., Matjafri, M.Z., Aziz, A.A. & Omar, A.F. (2014). Non-destructive
783 quality evaluation of fruit by color based on RGB LEDs system. Proceeding
784 of the 2nd International Conference on Electronic Design (ICED), 19–21, pg.
785 230.
786 Yahaya, O.K.M., MatJafri, M.Z., Aziz, A.A. & Omar, A.F. (2015). Visible
787 spectroscopy calibration transfer model in determining pH of Sala mangoes.
788 Journal of Instrumentation, 10, T05002.
789 Yashoda, H.M., Prabha, T.N. & mTharanathan, R.N. (2007). Mango ripening –
790 Role of carbohydrases in tissue softening. *Food Chemistry,* 102(3), 691-698.
791 Yashoda, H.M., Prabha, T.N. & Tharanathan, R.N. (2005). Mango ripening—
792 chemical and structural characterization of pectic and hemicellulosic
793 polysaccharides. *Carbohydrate research,* 340(7), 1335-1342.
794 Zakaria, A., Shakaff, A. Y. M., Masnan, M. J., Saad, F. S. A., Adom, A. H.,
795 Ahmad, M. N. & Kamarudin, L. M. (2012). Improved Maturity and Ripeness

796 Classifications of Magnifera Indica cv. Harumanis Mangoes through Sensor
797 Fusion of an Electronic Nose and Acoustic Sensor. *Sensors,*12(5), 6023–
798 6048.